EDGE-REFLECTION ANALYSIS OF GUIDED WAVES IN A 3-D PLATE

Arief Gunawan[1], Sohichi Hirose[1]

[1] Mechanical and Environmental Informatics, Tokyo Institute of Technology, Japan

Abstract

This study carries out the edge-reflection analysis of guided waves in a 3-D plate. First, we excite an incident guided wave by applying a normal traction on the surface of a 3-D plate. The excited wave field is obtained in the frequency and wavenumber domains. Secondly, we perform the edge-reflection analysis in the frequency and wavenumber domains by applying the mode-decomposition method to obtain the reflection coefficients as functions of the frequency and the wavenumber. Thirdly, the reflected waves are calculated in the frequency and wavenumber domains by using the reflection coefficients obtained in the second step. Lastly, we obtain the reflected waves in a 3-D plate by performing inverse Fourier transforms. The reflection coefficients in a 3-D plate are evaluated as the amplitude ratio between the reflected wave and the incident wave. We discuss the difference between the coefficients in 3-D and 2-D problems in detail by changing some parameters such as the size of the exciter and the distance between the exciter and the edge.

1. Introduction

Guided waves are the elastic waves which propagate in the longitudinal direction of waveguides such as a thin plate and a pipe. There are two types of guided waves propagating in a plate, namely Lamb waves and SH waves [1-3], which are guided waves of in-plane and anti-plane motions, respectively. A guided-wave ultrasonic method is usually applied in a nondestructive test to detect a defect in a waveguide. This method can be used to scan a wide range of a waveguide because the attenuation of guided waves is small. Since guided waves have several modes, most of which are dispersive, the characteristics of guided waves are, however, complicated. In order to improve the applicability of the guided-wave method in a plate, the clarification of the characteristics of guided waves is necessary. The reflection characteristic of guided waves by an edge of a plate is particularly important because the edge reflection is usually involved in practice.

The edge-reflection analyses of guided waves in a 2-D plate have been carried out in several studies [4-12]. Experiments have also been performed to verify analysis results [6, 13]. In a 2-D plate, the wave field is assumed to be uniform in the anti-plane direction. This assumption is rarely satisfied by the plate in practice since the width of the transmitting transducer is much smaller than the width of the plate. There is, therefore, difference between the reflection-analysis results in 2-D and 3-D plates. The objective of this study is to perform the reflection analysis in a 3-D plate and make a quantitative investigation of the difference between the reflection characteristics of guided waves in 2-D and 3-D plates.

The method of analysis in this study is divided into three steps. The first is an excitation analysis, in which the amplitudes of the guided waves excited by an external force applied on the surface of the plate are found. The second is the reflection analysis, in which the amplitudes of the reflected waves are evaluated. The first and second analyses are performed in the frequency and wavenumber domains. The second analysis is carried out by the mode-decomposition method [14]. The last step is the calculation of the reflection coefficients in a 3-D plate. The difference between the coefficients in 3-D and 2-D plates is discussed in detail by changing some parameters such as the size of the exciter and the distance between the exciter and the edge.

2. Review of the guided-wave theory in a 2.5-D plate

2.1. Fundamental relationships

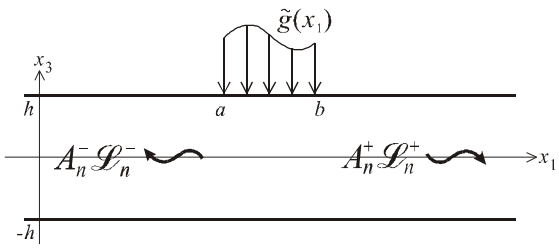

Figure 1: *Excitation of guided waves in a 2.5-D plate.*

Let us consider a homogeneous, isotropic, and linearly elastic plate as shown in Fig. 1. The wave

field in the plate is assumed to be harmonic with respect to the time t and an axis (x_2 in Fig. 1), i.e., the displacement can be expressed as follows:

$$\mathbf{u}(x_1, x_2, x_3, t) = \hat{\mathbf{u}}(x_1, x_3)e^{I(kx_2 - wt)} \tag{1}$$

where $I = \sqrt{-1}$, w is the frequency, x is the wavenumber in the x_2-direction. The thickness of the plate is $2h$ and the surfaces are assumed to be traction-free. In this paper, a plate with the wave field satisfying Eq. (1) is called a 2.5-D plate. There are two types of guided waves which propagate in the 2.5-D plate, i.e., Lamb waves and SH waves. The dispersion relations of symmetric and antisymmetric Lamb-wave modes and SH-wave modes are given by Eqs. (2), (3), and (4), respectively.

$$\frac{\tan(qh)}{\tan(ph)} + \frac{4k^2 pq}{(q^2 - k^2)^2} = 0 \tag{2}$$

$$\frac{\tan(qh)}{\tan(ph)} + \frac{(q^2 - k^2)^2}{4k^2 pq} = 0 \tag{3}$$

$$qh - \frac{np}{2} = 0 \tag{4}$$

where

$$p^2 = \frac{w^2}{c_L^2} - k^2 \qquad q^2 = \frac{w^2}{c_T^2} - k^2 \tag{5}$$

k is the wavenumber in the propagating direction, c_L and c_T are the velocities of the longitudinal and transverse waves, respectively, n is a non-negative integer. Dispersion curves of Lamb-wave and SH-wave modes for a steel plate (c_L =5940 m/s, c_T =3200 m/s) are shown in Fig. 2(a) and (b), respectively.

The general expressions of the displacements of guided waves in a 2.5-D plate are expressed as:

$$\begin{aligned}\mathbf{u}(x_1, x_2, x_3, t) &= \hat{\mathbf{u}}(x_1, x_3)e^{I(kx_2 - wt)} \\ &= \hat{\mathbf{u}}(x_3)e^{I(hx_1 + kx_2 - wt)}\end{aligned} \tag{6}$$

where

$$\hat{u}_1(x_3) = \frac{h}{k}\hat{U}_1(x_3) - \frac{x}{k}\hat{U}_2(x_3)$$

$$\hat{u}_2(x_3) = \frac{x}{k}\hat{U}_1(x_3) + \frac{h}{k}\hat{U}_2(x_3)$$

$$\hat{u}_3(x_3) = \hat{U}_3(x_3)$$

$$h = \sqrt{k^2 - x^2}$$

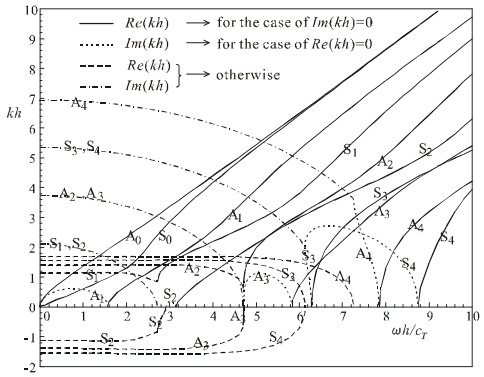

(a)

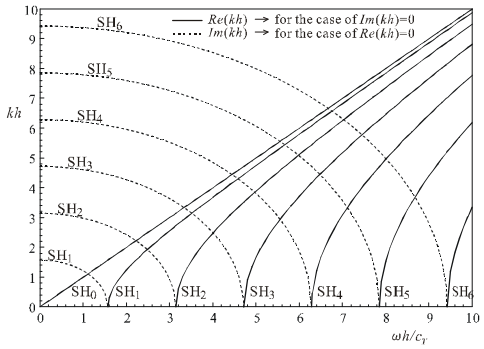

(b)

Figure 2: *Dispersion curves of (a) Lamb-wave modes and (b) SH-wave modes.*

The expression of $\hat{U}_i$ depends on the type of the guided wave. $\hat{U}_i$ for symmetric and antisymmetric Lamb-wave modes, and symmetric and antisymmetric SH-wave modes are given by Eqs. (7)-(10), respectively.

$$\begin{cases} \hat{U}_1(x_3) = IAk\left[\dfrac{\cos(px_3)}{\sin(ph)} + \dfrac{2pq}{k^2 - q^2}\dfrac{\cos(qx_3)}{\sin(qh)}\right] \\ \hat{U}_2(x_3) = 0 \\ \hat{U}_3(x_3) = -Ap\left[\dfrac{\sin(px_3)}{\sin(ph)} - \dfrac{2k^2}{k^2 - q^2}\dfrac{\sin(qx_3)}{\sin(qh)}\right] \end{cases} \tag{7}$$

$$\begin{cases} \hat{U}_1(x_3) = IAk\left[\dfrac{\sin(px_3)}{\cos(ph)} + \dfrac{2pq}{k^2 - q^2}\dfrac{\sin(qx_3)}{\cos(qh)}\right] \\ \hat{U}_2(x_3) = 0 \\ \hat{U}_3(x_3) = Ap\left[\dfrac{\cos(px_3)}{\cos(ph)} - \dfrac{2k^2}{k^2 - q^2}\dfrac{\cos(qx_3)}{\cos(qh)}\right] \end{cases} \tag{8}$$

$$\begin{cases} \hat{U}_1(x_3) = \hat{U}_3(x_3) = 0 \\ \hat{U}_2(x_3) = Ak\cos(qx_3) \end{cases} \tag{9}$$

$$\begin{cases} \hat{U}_1(x_3) = \hat{U}_3(x_3) = 0 \\ \hat{U}_2(x_3) = Ak\sin(qx_3) \end{cases} \tag{10}$$

where A is a constant. The stress t can be found by Eq. (11).

$$t_{ij} = r(c_L^2 - 2c_T^2)u_{k,k}d_{ij} + rc_T^2(u_{i,j} + u_{j,i}) \quad (11)$$

where r is the density.

2.2. Orthogonality of guided-wave modes

Hereafter, guided-wave modes including symmetric and antisymmetric Lamb waves and SH waves are denoted by L_1, L_2, … and the wavenumber of L_i is denoted by k_i. Let two arbitrary modes have the displacements and stresses [**u**, **τ**] and [**v**, **σ**], respectively, where

$$\begin{aligned}
\mathbf{u} &= \hat{\mathbf{u}}e^{I(xx_2-wt)} = \hat{\mathbf{u}}e^{I(h_m x_1 + x x_2 - wt)} \\
\boldsymbol{\tau} &= \hat{\boldsymbol{\tau}}e^{I(xx_2-wt)} = \hat{\boldsymbol{\tau}}e^{I(h_m x_1 + x x_2 - wt)} \\
\mathbf{v} &= \hat{\mathbf{v}}e^{I(xx_2-wt)} = \hat{\mathbf{v}}e^{I(h_n x_1 + x x_2 - wt)} \\
\boldsymbol{\sigma} &= \hat{\boldsymbol{\sigma}}e^{I(xx_2-wt)} = \hat{\boldsymbol{\sigma}}e^{I(h_n x_1 + x x_2 - wt)}
\end{aligned} \quad (12)$$

The orthogonality of guided-wave modes in a 2.5-D plate is described as

$$(h_m - h_n^*)P_{mn}^x = 0 \quad (13)$$

where the superscript * denotes the complex conjugate and

$$P_{mn}^x = \frac{Iw}{4}\int_{-h}^{h}(\hat{u}_i\hat{s}_{1i}^* - \hat{v}_i^*\hat{t}_{1i})dx_3 \quad (14)$$

According to Eq. (13), P_{mn}^x is always zero when $h_m = h_n^*$. For simplification, we define $Q_m^x = P_{mn}^x$ for the case of $h_m = h_n^*$.

2.3. Mode decomposition

Here a method to decompose an arbitrary wave field in a 2.5-D plate into the superposition of guided-wave modes using the orthogonal property shown above is presented. Let the displacement and stress of the wave field E to be decomposed be [$\hat{\mathbf{u}}e^{I(xx_2-wt)}$, $\hat{\boldsymbol{\tau}}e^{I(xx_2-wt)}$]. For simplification, we define a new operator $\circ$ as follows:

$$E \circ E' \equiv \frac{Iw}{4}\int_{-h}^{h}(\hat{u}_i\hat{s}_{1i}^* - \hat{v}_i^*\hat{t}_{1i})dx_3 \quad (15)$$

where E=[$\hat{\mathbf{u}}e^{I(xx_2-wt)}$, $\hat{\boldsymbol{\tau}}e^{I(xx_2-wt)}$] and E'=[$\hat{\mathbf{v}}e^{I(xx_2-wt)}$, $\hat{\boldsymbol{\sigma}}e^{I(xx_2-wt)}$]. From Eqs. (12) and (14), it is clear that $L_m \circ L_n$ is equal to P_{mn}^x. We also define a function $n = g(m)$ that relates m to n so that $h_n = h_m^*$.

When E is expressed as the superposition of guided-wave modes as Eq. (16), the amplitude of each mode A_m can be found by Eq. (17).

$$E = \sum_{m=1}^{\infty} A_m L_m \quad (16)$$

$$A_m = \frac{E \circ L_{g(m)}}{Q_m^x} \quad (17)$$

2.4. Excitation of guided waves

When an external force is applied on the surface of a 2.5-D plate, the amplitudes of the excited guided-wave modes can be analytically found by the reciprocity theorem. Assume that an external force $g(x_1)$ is applied normally to the surface of the plate as shown in Fig. 1. Guided-wave modes are excited and propagate to the left and right directions. Let the modes which propagate to the left and right directions be denoted by L_n^- and L_n^+, respectively. To relate the index n in $L_n^{\pm}$ to the index m in L_m, we define functions $f^{\pm}(n)$ in such a way that $L_n^{\pm} \equiv L_m$ if $m = f^{\pm}(n)$.

The amplitudes $A_n^{\pm}$ of the excited modes $L_n^{\pm}$ can be found as

$$A_n^{\pm} = \frac{Iw}{4Q_n^x}\int_a^b g(x_1)\left[\hat{u}_3^{g\{f^{\pm}(n)\}}(x_1, h)\right]^* dx_1 \quad (18)$$

where $\mathbf{u}^m$ is the displacement of L_m mode [see Eq. (6)].

3. Statement of the problem

The problem is illustrated in Fig. 3. When the external normal force $f(t)g(x_1, x_2)$ is applied to the surface of the semi-infinite 3-D plate, the incident wave $\mathbf{u}^{(\mathrm{in})}$ is excited and reflected by the free edge S_e of the plate as $\mathbf{u}^{(\mathrm{ref})}$. The problem in this study is to find $\mathbf{u}^{(\mathrm{in})}$ and $\mathbf{u}^{(\mathrm{ref})}$ and evaluate the reflection coefficients in a 3-D plate.

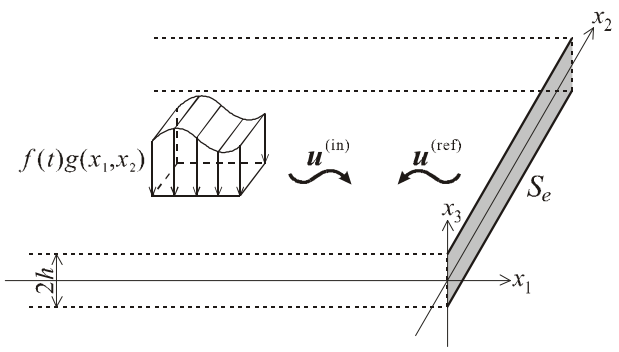

Figure 3: *Problem statement.*

4. Analysis method

The outline of the analysis method is shown in Fig. 4. First, the external force $f(t)g(x_1, x_2)$ in the time and space domains is Fourier transformed (FFT)

into the external force $\tilde{f}(w)\tilde{g}(x_1,x)$ in the frequency and wavenumber domains. In each frequency and each wavenumber, the amplitudes $A_n^+(w,x)$ of all excited modes L_n^+ are found. The wave $\sum A_n^+(w,x)L_n^+$ is the incident wave to the free edge of the 2.5-D plate. The amplitudes $A_n^-(w,x)$ of all reflected modes are evaluated by using the reflection coefficients in a 2.5-D plate, which are obtained from the reflection analysis in a 2.5-D plate. The superposition of these modes $\sum A_n^-(w,x)L_n^-$ becomes the reflected wave $\tilde{\mathbf{u}}^{(\mathrm{ref})}(x_1,x,x_3,w)$ in the frequency and wavenumber domains. When the inverse Fourier transform is applied to $\tilde{\mathbf{u}}^{(\mathrm{ref})}(x_1,x,x_3,w)$, the reflected wave $\mathbf{u}^{(\mathrm{ref})}(x_1,x_2,x_3,t)$ in the time and space domains is found. The obtained wave is processed to find the reflection coefficients in a 3-D plate. In sequence, the excitation analysis in a 2.5-D plate, the reflection analysis in a 2.5-D plate, and the reflection analysis in a 3-D plate are discussed, whereas the details of FFT and inverse FFT are skipped in this paper.

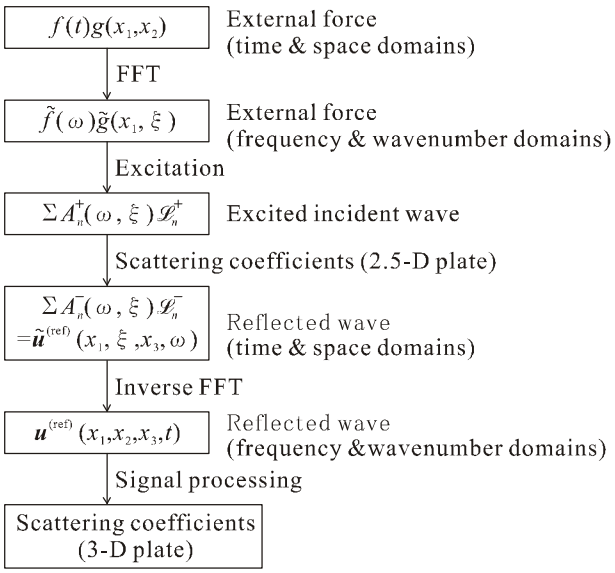

Figure 4: *Procedure to find the reflection coefficients in a 3-D plate.*

4.1. Excitation analysis in a 2.5-D plate

According to Eq. (18), the amplitude $A_n^+(w,x)$ of the L_n^+ mode excited by the external force $\tilde{f}(w)\tilde{g}(x_1,x)$ is given as

$$A_n^+(w,x)=\frac{Iw\,\tilde{f}(w)}{4Q_n^x}\int_a^b \tilde{g}(x_1,x)\left[\tilde{u}_3^{g\{f^+(n)\}}(x_1,h)\right]^* dx_1 \quad (19)$$

4.2. Reflection analysis in a 2.5-D plate

The reflection problem in a 2.5-D plate is illustrated in Fig. 5. In the reflection analysis, the amplitudes r_m^n of all reflected modes L_n^- due to the incident wave of the L_n^+ mode with unit amplitude are to be determined. In this study, the reflection analysis is carried out by applying the mode-decomposition method shown in Sec. 2.3.

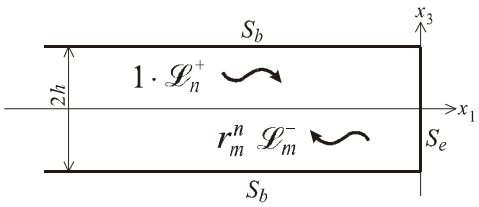

Figure 5: *Reflection of a guided wave by an edge of a 2.5-D plate.*

Let the displacement and stress of the total wave in reflection problem shown in Fig. 5 be [**v**, **σ**] and those of the L_n mode be [$\mathbf{u}^n$, $\boldsymbol{\sigma}^n$]. Since [**v**, **σ**] is the superposition of $1\cdot L_n^+$ and $r_m^n\cdot L_m^-$, [**v**, **σ**], [$\mathbf{u}^n$, $\boldsymbol{\sigma}^n$], and r_m^n can be related to each other by Eq. (17). In fact, after substituting [**v**, **σ**] to E, $f^-(l)$ to m, and r_l^n to A_m into Eq. (17), Eq. (20) can be obtained.

$$r_l^n=\frac{Iw}{4Q_{f^-(l)}^x}\int_{-h}^{h}\left[\tilde{v}_i\left\{\tilde{t}_{1i}^{g\{f^-(l)\}}\right\}^*-\left\{\tilde{u}_i^{g\{f^-(l)\}}\right\}^*\tilde{s}_{1i}\right]dx_3 \quad (20)$$

Let consider Eq. (20) for x_1=0, which is the location of the edge. Since the edge is traction-free, we have the relation of $\tilde{s}_{1i}\equiv 0$ for the stress components of the total wave. The displacement of the total wave can be represented as the superposition of the incident and reflected waves.

$$\mathbf{v}=\mathbf{u}^{f^+(n)}+\sum_m r_m^n\mathbf{u}^{f^-(m)} \quad (21)$$

And also we have $\tilde{v}_i\left\{\tilde{t}_{1i}^{g\{f^-(l)\}}\right\}^*=\hat{v}_i\left\{\hat{t}_{1i}^{g\{f^-(l)\}}\right\}^*$ at x_1=0. Eq. (20) then becomes

$$\sum_m\left[\int_{-h}^{h}\hat{u}_i^{f^-(m)}\left\{\hat{t}_{1i}^{g\{f^-(l)\}}\right\}^*dx_3-\frac{4Q_{f^-(l)}^x}{Iw}d_{lm}\right]r_m^n \quad (22)$$
$$=-\int_{-h}^{h}\hat{u}_i^{f^+(m)}\left\{\hat{t}_{1i}^{g\{f^-(l)\}}\right\}^*dx_3$$

The unknowns in Eq. (22) are r_m^n (m=1,2,…). Because Eq. (22) is valid for l=1,2,…, these equations can be simultaneously solved to find r_m^n. The amplitudes A_n^- of the reflected mode L_n^- can be evaluated as

$$A_n^- = \sum_m A_m^+ r_n^m \tag{23}$$

4.3. Reflection analysis in a 3-D plate

The reflection coefficients in a 3-D plate are evaluated as follows. We consider a semi-infinite 3-D plate as shown in Fig. 6(a). The external force is applied at point C on the surface of the plate. $U^{(\mathrm{ref})}(x_1,t)$, which is the x_3-component of the displacement of the reflected wave, is numerically measured at equally spaced *N* points on AB range on the surface of the plate. As reference wave, $U^{(\mathrm{rfr})}(x_1,t)$, which is the x_3-component of the displacement of the wave propagating in an infinite 3-D plate as shown in Fig. 6(b), is measured at equally spaced *N* points on AB range.

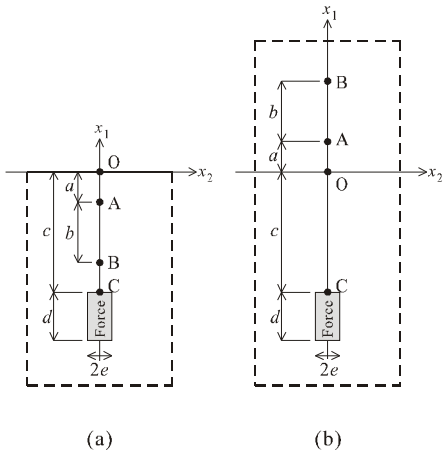

Figure 6: *Measurement setup of (a) reflected wave in a semi-infinite plate and (b) reference wave in an infinite plate*

$U^{(\mathrm{ref})}(x_1,t)$ and $U^{(\mathrm{rfr})}(x_1,t)$ are Fourier transformed with respect to x_1 and t to obtain the amplitudes $\tilde{U}^{(\mathrm{ref})}(k,w)$ and $\tilde{U}^{(\mathrm{rfr})}(k,w)$ in the wavenumber and frequency domains [15]. The reflection coefficients in a 3-D plate are defined as follows:

$$\left|r_n^n\right| = \frac{\tilde{U}^{(\mathrm{ref})}\{k^n(w),w\}}{\tilde{U}^{(\mathrm{rfr})}\{k^n(w),w\}} \tag{24}$$

where $k^n(w)$ is the wavenumber of the L_n mode at the frequency w .

5. Analysis results

5.1. Numerical implementation

In the analysis shown later, the temporal function of the external force *f*(*t*) shown in Eq. (25) is adopted. Fig. 7 illustrates the force.

$$f(t) = \sin(w_c) H_w(t) \tag{25}$$

$$H_w(t) = \begin{cases} 0.5 - 0.5\cos(2pt/t_1), & 0 \le t \le t_1 \\ 0, & \text{otherwise} \end{cases} \tag{26}$$

In the following analysis result, $w_c h / c_T = 1$ and $t_1 w_c = 10p$ are adopted. At the frequency $w_c h / c_T = 1$, there exist two propagating Lamb-wave modes (A_0 and S_0) and a propagating SH-wave mode (SH_0) as shown in Fig. 2. The Fourier transform of *f*(*t*) is carried out by considering 512 points of time in the time range of $0 \le t w_c \le 300$.

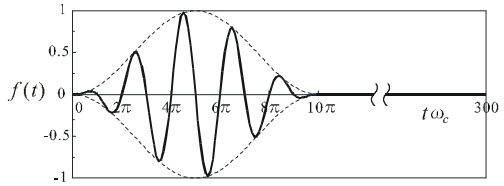

Figure 7: *Function f(t) which is used as the external force.*

The spatial function of the external force $g(x_1,x_2)$ is taken as Eq. (27).

$$g(x_1,x_2) = e^{Ik^n x_1} H_{[-c-d,-c]}(x_1) H_{[-e,e]}(x_2) \tag{27}$$

$$H_{[a,b]}(x) = \begin{cases} 1, & a \le x \le b \\ 0, & \text{otherwise} \end{cases} \tag{28}$$

where k^n is the wavenumber at the frequency $w = w_c$ of the mode L_n which is intended to be excited. The position of the force is shown in Fig. 6. The Fourier transform of $g(x_1,x_2)$ with respect to x_2 is carried out by considering 2048 points of x_2 in the range of $-128l \le x_2 \le 128l$, where l is the wavelength of the L_n mode.

In all results shown later, the values of *b* and *d* in Fig. 6 are fixed to $b/l = 4$ and $d/l = 5$. The waveforms at 32 points on AB range are used in calculating the reflection coefficients in a 3-D plate.

5.2. Verification of the excitation analysis result

The verification of the excitation analysis result is carried out by comparison with the analytical result [16] for a 3-D plate. Fig. 8 shows the displacement u_3 measured on x_1-axis in Fig. 6(b). The external force is chosen so as to excite the S_0 mode. $w_c h / c_T = 1$, $a/l = 10$, $c/l = 50$, $e/l = 0.5$ are selected. The curves with circles and those with squares represent the 2.5-D analysis result and the exact solution, respectively. The error between them is found less that 0.2%. The excitation analysis and the FFT with respect to time and space used in this study are then verified.

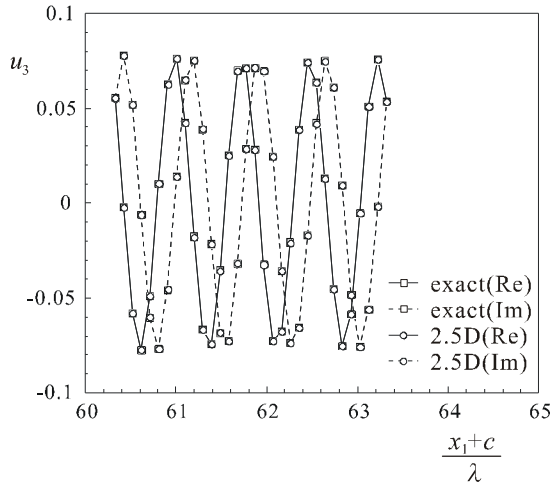

Figure 8: *Comparison between the exact solution and the 2.5-D analysis result. (Re=real part, Im=imaginary part)*

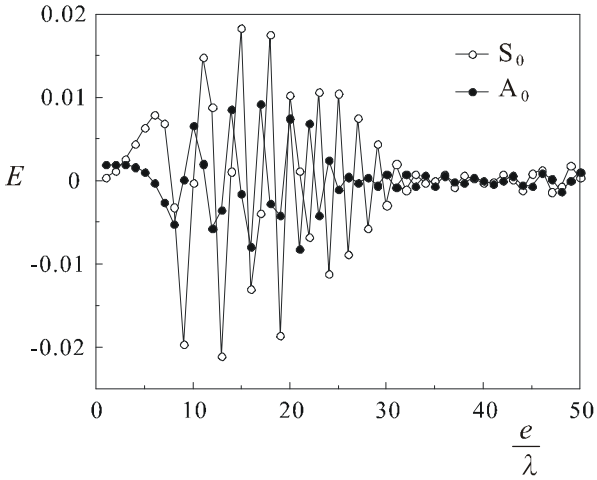

Figure 9: *Difference E as a function of* e/l .

5.3. Comparison between the reflection coefficients in 3-D and 2-D plates

Generally, the larger the width 2e of the external force is, the more similar the 3-D plate is to the 2-D plate. We will investigate first the dependency on e/l of the difference E between the reflection coefficients for 3-D and 2-D plates. The difference E is defined as follows:

$$E = \frac{|r_n^n| - |R_n^n|}{|r_n^n|} \tag{29}$$

where r_n^n and R_n^n are the reflection coefficients for 3-D and 2-D plates, respectively. The relations between E and e/l are shown in Fig. 9 for the A_0 and S_0 modes incidences. Here, $w_c h/c_T = 1$, $a/l = 1$ and $c/l = 40$ are adopted. Note that the reflection coefficients R_n^n are equal to unity at this frequency. From this figure, it is found that E for both A_0 and S_0 modes incidences are small at quite small e/l . As e/l increases, E becomes larger, but E almost vanishes at e/l larger than a value ($\approx$ 35). This behavior is also observed for other c/l as shown in Fig. 10. Figs. 10(a) and (b) show the value of E as a function of c/l and e/l for the A_0 and S_0 modes, respectively. It is also seen that the value of e/l from which E vanishes becomes larger as c/l increases. In this region of e/l , the 3-D reflection problem is closely similar to the 2-D reflection problem. By comparing figures (a) and (b), we also find the distinction in magnitude of E for A_0 and S_0 incidences. The magnitude of E for the S_0 incidence is larger than that for the A_0 incidence because the reflection problem for the A_0 incidence involves only a mode whereas that for the S_0 incidence involves two modes (S_0 and SH_0).

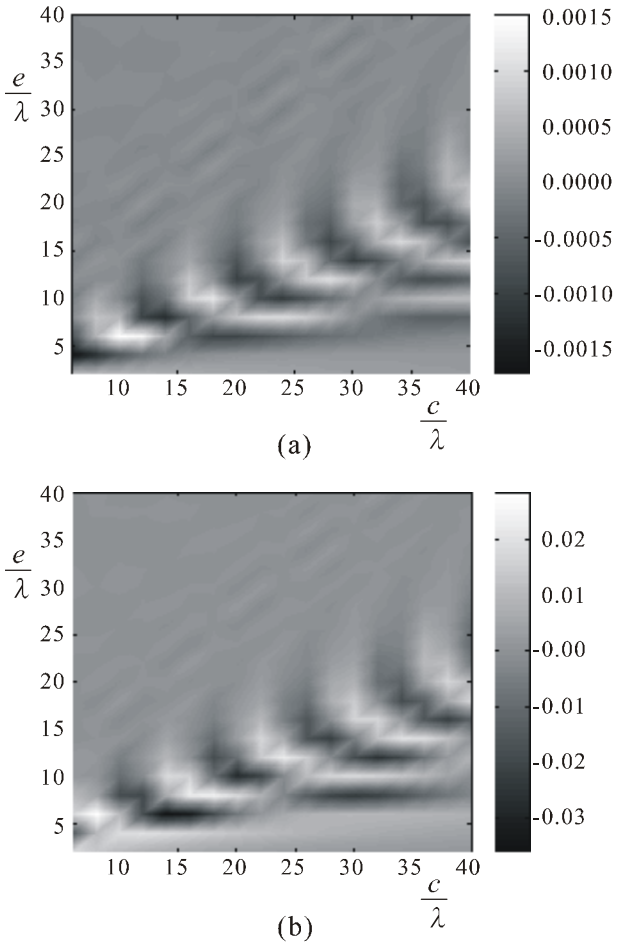

Figure 10: *Difference E as a function of* c/l *and* e/l *for (a)* A_0 *mode and (b)* S_0 *mode incidences.*

Let us discuss the cause of the large difference E observed in Fig. 10. Figs. 11, 12, and 13 show the time-series displacement fields u_3 when the S_0 mode

is incident to the edge for the cases of e/l =15, 5, and 1, respectively. The value of c/l is fixed to 10. The times tw_c of the figures (a)-(d) are 46.4, 64.0, 80.4, and 128.6, respectively. The figures (a), (b), and (c) show the incident wave propagating toward the edge (x_1=0) and the figure (d) the reflected wave propagating away from the edge. Note that the SH_0 mode does not appear in these figures because its displacement does not have x_3-component. In the case of e/l =15 (Fig. 11), since the width of the external force is quite large, the S_0 mode is excited with a wide uniform region centered at x_2/l =0. Although some disturbance appears around $x_2/l = \pm 15$ as the S_0 mode propagates toward the edge, a wide uniform region of wave field still exists when the mode is reflected by the edge. In the case of e/l =5 (Fig. 12), although a uniform region of wave field appears just after the S_0 mode is excited, the uniform region shrinks as the S_0 mode propagates and disappears after the S_0 mode is reflected by the edge. The disappearance of uniform region causes large difference E for the case c/l =10, e/l =5. In the case of e/l =1 (Fig. 13), no uniform region of wave field appears at first, but as the S_0 mode propagates the wave front becomes flat gradually and a locally uniform region is constructed, which is the reason why the difference E is small for e/l =1.

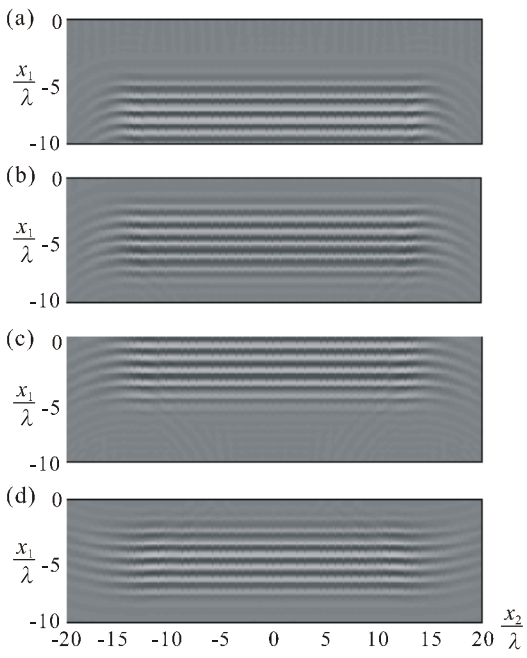

Figure 11: *Time-series wave fields of S_0 mode incidence for e/l =15.*

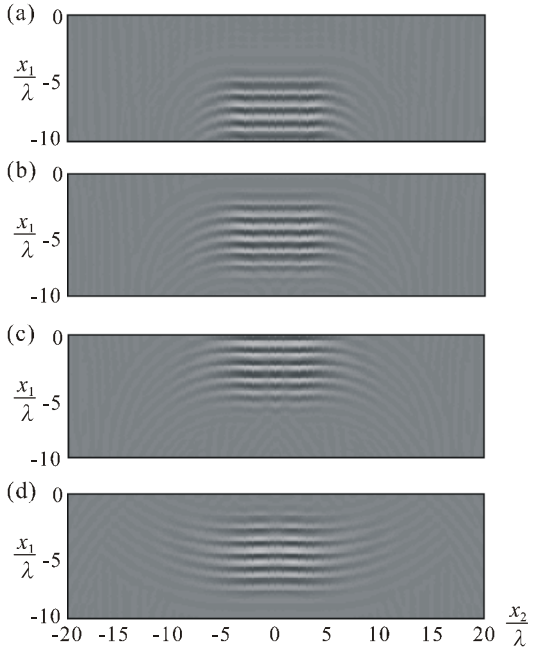

Figure 12: *Time-series wave fields of S_0 mode incidence for e/l =5.*

As mentioned above, small difference E is obtained for small e/l. In such a case, the effect of a/l and c/l on E is also of interest. Fig. 14 shows the relation between E and a/l for e/l =1, c/l =40. It is found that E decreases as a/l increases, nevertheless E is less sensitive to the change of a/l. Fig. 15 shows the dependency of E to c/l when e/l =1, a/l =1. It is observed that E becomes large for small c/l. The reason is that the curvature of the wave front is still large when the S_0 mode is reflected by the edge. As c/l increases, the curvature becomes smaller and E decreases.

6. Conclusions

The excitation analysis by an external force and the edge-reflection analysis in a semi-infinite 3-D plate were carried out. The obtained waveforms are utilized to find the scattering coefficients in a 3-D plate, which are compared to the scattering coefficients in a 2-D plate. The effect of some parameters such as the width of the external force, the distance between the external force and the edge, and the location of measurement, to the difference between the scattering coefficients in 3-D and 2-D plates was investigated. It was found that the difference can be reduced by enlarging the width of the external force or using an external force with quite narrow width.

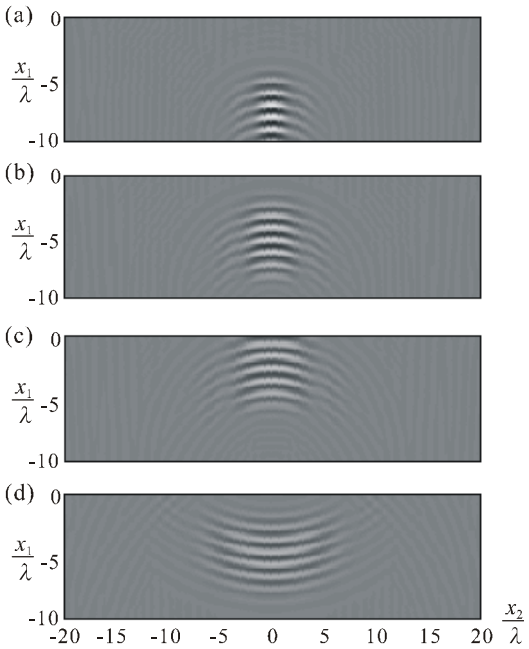

Figure 13: *Time-series wave fields of S_0 mode incidence for e/l =1.*

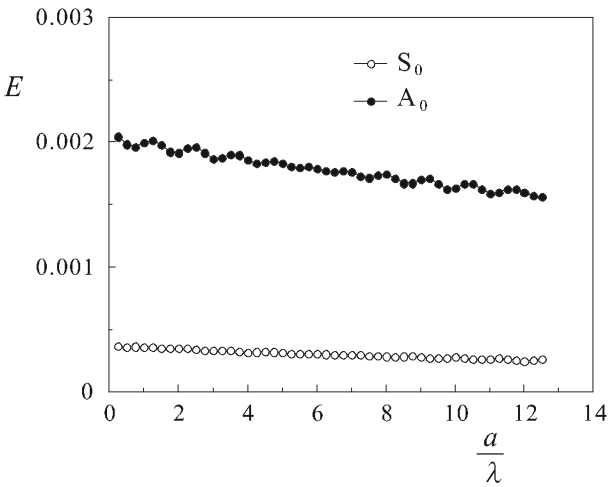

Figure 14: *Difference E as a function of a/l .*

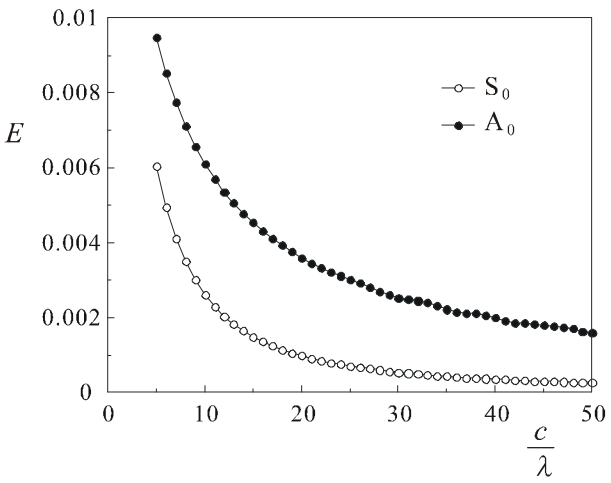

Figure 15: *Difference E as a function of c/l .*

7. References

[1] I. A. Viktorov, *Rayleigh and Lamb Waves: Physical Theory and Application*, Plenum, New York, 1967.

[2] B. A. Auld, *Acoustic Fileds and Waves in Solids*, John Wiley and Sons, New York, 1973.

[3] J. D. Achenbach, *Wave Propagation in Elastic Solids*, North-Holland, Amsterdam, 1973.

[4] P. J. Torvik, Reflection of Wave Trains in Semi-Infinite Plates, *J. Acous. Soc. Am.* 41: 346-353, 1967.

[5] B. A. Auld and E. M. Tsao, Variational analysis of edge resonance in a semi-infinite plate, *IEEE Trans. Sonics Ultrason.* SU-24, 5: 317-326, 1977.

[6] B. Morvan, N. Wilkie-Chancellier, H. Duflo, A. Tinel, and J. Duclos, Lamb wave reflection at the free edge of a plate, *J. Acoust. Soc. Am.* 113: 1417-1425, 2003.

[7] N. Wilkie-Chancellier, H. Duflo, A. Tinel, and J. Duclos, Numerical description of the edge mode at the beveled extremity of a plate, *J. Acoust. Soc. Am.* 117: 194-199, 2005.

[8] R. D. Gregory and I. Gladwell, The reflection of symmetric Rayleigh-Lamb wave at the fixed or free edge of a plate, *J. Elast.* 13: 185-206, 1983.

[9] M. Koshiba, Finite-element analysis of edge resonance in a semi-infinite elastic plate, *Electron. Lett.* 19: 256-257, 1983.

[10] J. M. Galan and R. Abascal, Numerical simulation of Lamb wave scattering in semi-infinite plates, *Int. J. Numer. Meth. Engng.* 53: 1145-1173, 2002.

[11] Y. H. Cho and J. L. Rose, A boundary element solution for a mode conversion study on the edge reflection of Lamb waves, *J. Acous. Soc. Am.* 99: 2097-2109, 1996.

[12] A. Gunawan and S. Hirose, Mode-exciting method for Lamb wave-scattering analysis, *J. Acoust. Soc. Am.* 115: 996-1005, 2004.

[13] N. Wilkie-Chancellier, H. Duflo, A. Tinel, and J. Duclos, Experimental study and signal analysis in the Lamb wave conversion at a bevelled edge, *Ultrason.* 42: 377-381, 2004.

[14] A. Gunawan and S. Hirose, Reflection of Obliquely Incident Lamb waves and SH waves by an Edge of a Plate (*to be published*).

[15] D. Alleyne and P. Cawley, A two-dimensional Fourier transform method for the measurement of propagating multimode-signals, *J. Acoust. Soc. Am.* 89: 1159-1168, 1991.

[16] J. D. Achenbach and Y. Xu, Wave motion in an isotropic elastic layer generated by a time-harmonic point load of arbitrary direction, *J. Acous. Soc. Am.* 106: 83-90, 1999.

Acknowledgments

This work was supported by Grant-in Aid of the Ministry of Education, Culture, Sports, Science and Technology, and the Japan Society for the Promotion of Science.